

# Combinatorial strategies targeting NEAT1 and AURKA as new potential therapeutic options for multiple myeloma

Noemi Puccio,<sup>1,2</sup> Gloria Manzotti,<sup>1</sup> Elisabetta Mereu,<sup>3</sup> Federica Torricelli,<sup>1</sup> Domenica Ronchetti,<sup>4</sup> Michela Cumerlato,<sup>3</sup> Ilaria Craparotta,<sup>5</sup> Laura Di Rito,<sup>5</sup> Marco Bolis,<sup>5,6</sup> Valentina Traini,<sup>4</sup> Veronica Manicardi,<sup>1</sup> Valentina Fragliasso,<sup>1</sup> Yvan Torrente,<sup>7,8</sup> Nicola Amodio,<sup>9</sup> Niccolò Bolli,<sup>4,10</sup> Elisa Taiana,<sup>10</sup> Alessia Ciarrocchi,<sup>1</sup> Roberto Piva<sup>3</sup> and Antonino Neri<sup>11</sup>

<sup>1</sup>Laboratory of Translational Research, Azienda USL-IRCCS di Reggio Emilia, Reggio Emilia, Italy; <sup>2</sup>Clinical and Experimental Medicine PhD Program, University of Modena and Reggio Emilia, Modena, Italy; <sup>3</sup>Department of Molecular Biotechnology and Health Sciences, University of Turin, Turin, Italy; <sup>4</sup>Department of Oncology and Hemato-Oncology, University of Milan, Milan, Italy; <sup>5</sup>Computational Oncology Unit, Oncology Department, Mario Negri IRCCS, Milan, Italy; <sup>6</sup>Bioinformatics Core Unit, Institute of Oncology Research (IOR), Bellinzona, Switzerland; <sup>7</sup>Stem Cell Laboratory, Dino Ferrari Center, Department of Pathophysiology and Transplantation, University of Milan, Milan, Italy; <sup>8</sup>Neurology Unit, Fondazione IRCCS Cà Granda Ospedale Maggiore Policlinico, Milan, Italy; <sup>9</sup>Department of Experimental and Clinical Medicine, Magna Graecia University of Catanzaro, Catanzaro, Italy; <sup>10</sup>Hematology Unit, Fondazione IRCCS Cà Granda Ospedale Maggiore Policlinico, Milan, Italy and <sup>11</sup>Scientific Directorate, Azienda USL-IRCCS di Reggio Emilia, Reggio Emilia, Italy

**Correspondence:** A. Neri  
[antonino.neri@ausl.re.it](mailto:antonino.neri@ausl.re.it)

**Received:** March 22, 2024.

**Accepted:** July 2, 2024.

**Early view:** July 11, 2024.

<https://doi.org/10.3324/haematol.2024.285470>

©2024 Ferrata Storti Foundation

Published under a CC BY-NC license



## Supplementary Methods

### Combinatorial strategies targeting NEAT1 and AURKA as new potential therapeutic options for Multiple Myeloma

#### Authors:

Noemi Puccio<sup>1,2</sup>, Gloria Manzotti<sup>1</sup>, Elisabetta Mereu<sup>3</sup>, Federica Torricelli<sup>1</sup>, Domenica Ronchetti<sup>4</sup>, Michela Cumerlato<sup>3</sup>, Ilaria Craparotta<sup>5</sup>, Laura Di Rito<sup>5</sup>, Marco Bolis<sup>5,6</sup>, Valentina Traini<sup>4</sup>, Veronica Manicardi<sup>1</sup>, Valentina Fragliasso<sup>1</sup>, Yvan Torrente<sup>7</sup>, Nicola Amodio<sup>8</sup>, Niccolò Bolli<sup>4,9</sup>, Elisa Taiana<sup>9</sup>, Alessia Ciarrochi<sup>1</sup>, Roberto Piva<sup>3</sup>, Antonino Neri<sup>10</sup>.

<sup>1</sup>Laboratory of Translational Research, Azienda Unità Sanitaria Locale-IRCCS Reggio Emilia, Reggio Emilia; <sup>2</sup>Clinical and Experimental Medicine PhD Program, University of Modena and Reggio Emilia, Modena; <sup>3</sup>Department of Molecular Biotechnology and Health Sciences, University of Turin, Turin, Italy, <sup>4</sup>Department of Oncology and Hemato-Oncology, University of Milan, Milan, Italy, <sup>5</sup>Computational Oncology Unit, Oncology Department, Mario Negri IRCCS, Milan, <sup>6</sup>Bioinformatics Core Unit, Institute of Oncology Research (IOR), Bellinzona, Switzerland.; Università della Svizzera Italiana, Faculty of Biomedical Sciences, 6900 Lugano, Switzerland, <sup>7</sup>Stem Cell Laboratory, Department of Pathophysiology and Transplantation, University of Milan, Centro Dino Ferrari, Unit of Neurology, Fondazione IRCCS Cà Granda Ospedale Maggiore Policlinico, 20122 Milan, Italy; Novsystem Spa, Milan, <sup>8</sup>Department of Experimental and Clinical Medicine, Magna Graecia University of Catanzaro, Catanzaro, <sup>9</sup>Hematology, Fondazione IRCCS Cà Granda Ospedale Maggiore Policlinico, Milan, Italy, <sup>10</sup>Scientific Directorate, Azienda USL-IRCCS Reggio Emilia, 42123 Reggio Emilia, Italy.

## Gymnosis

Cells were seeded at low plating density ( $5 \times 10^4$ /ml) and concurrently treated with the naked gapmeR NEAT1 (gNEAT1) and the scrambled (gSCR), at a final concentration of 1.5, 2.5, 5, 7  $\mu$ M. Table showing the LNA-gapmeRs used:

Name	Sequence ( 5' - 3' )	Mw calc (Da)
<b>gNEAT1</b>	AGTGACCACAAAAGGT	5276.2
<b>gSCR</b>	GCTCCCTTCAATCCAA	5184.2

## Drug synergism analysis

For HT experiments, Growth Rate (GR) was calculated as the ratio between luminescence values at the two time points, normalized to DMSO-treated cells. Combined drug effect was determined by Excess over Bliss (EOB) analysis on GR value for all concentrations, according to the formula:

$$EOB = [1 - GR(\text{combination})] - [1 - GR(\text{DMSO})] - [1 - GR(\text{drug})] + [1 - GR(\text{DMSO})][1 - GR(\text{drug})]^2$$
. EOB cut off  $>0.2$  was used to select the most synergistic drugs (TOP35) in combination with NEAT1 KD.

During the validation step, drug combination studies and synergy quantification were realized with CompuSyn software based on Chou-Talalay method that calculates the combination index (CI). Dose-effect curves were determined by counting viable cells after 72 hours of Alisertib and AURKAI-I treatment and 96 hours after NEAT1 silencing. At least three different concentrations of each drug were combined to two concentrations of gNEAT1 gapmeR (2,5 – 7  $\mu$ M)

## Cell cycle analysis

Cell cycle analyses were performed in AMO-1, NCI-H929 and MM1.S cells after 24 hours of Alisertib and AURKAI-I treatments. Cells were analyzed with the hypotonic propidium iodide (PI) method<sup>1</sup> and samples were acquired with FACS Canto II Cell Analyzer (BD Biosciences).

### **Cell viability assessment**

MM cells proliferation was assessed through Trypan-exclusion method and live cell imaging.

### **Live cell imaging and analysis**

For proliferation assays, cells were seeded in coated 96-well plates (4000 cells/well). Cell coating was performed using 50  $\mu\text{L}$  of 0.005% Poly-L-ornithine solution per well. The plate was incubated for 1 hour at room temperature then, poly-L-ornithine solution was removed from the well to allow the plate to dry for 15 minutes. Cells were stained for 20 minutes at 37  $^{\circ}\text{C}$  using 0,5  $\mu\text{M}$  Citolight Red (4706) (Sartorius AG, Goettingen, Germany), resuspended in PBS 1X. Then, cells were centrifuged at 900 rpm for 5 minutes and resuspended in the appropriate amount of standard medium supplemented with different drugs.

Cell proliferation analysis was performed with the Incucyte<sup>®</sup> Live-Cell Analysis Systems (Model S3; Sartorius AG, Goettingen, Germany). Cells were imaged within 20 minutes of plating using phase contrast and red (400 ms exposure) image channels in the Incucyte<sup>®</sup> platform. Five images from distinct regions per well using a 10x dry objective lens were taken every 8 hours. Independent experimental condition was run in triplicates. The InCuCyte software's analysis definition was set to recognize red-stained cells. Top-Hat segmentation method was used for background correction. For accurate quantification of closely spaced objects edge split tool was used. Cell objects count was finalized by applying specific filter for each cell line:  $<120 \mu\text{m}^2$  for AMO-1 and for NCI-H929 and  $<110 \mu\text{m}^2$  for MM1.S cells. Red object counts per image, for all the five images acquired in each independent technical replicate were used to determine the average number of cells per well.

### **RNA extraction, reverse transcription and quantitative PCR**

Total RNA was extracted using RNeasy kit (Qiagen) according to manufacturer's instructions. The purity and concentration of total RNA was determined by the NanoDrop 1000 spectrophotometer (Thermo Fisher Scientific). The ratios of absorption (260 nm/280 nm) of all samples were between 1.8 and 2.0. 500 ng of total RNA was retrotranscribed with iScript cDNA kit (Bio-Rad, Hercules, California, USA). Quantitative Real-Time PCR (qRT-PCR) was performed for 40 cycles using Sso Fast EvaGreen Super Mix (Bio-Rad, Hercules, California, USA) in a CFX96 Real Time PCR Detection System (Bio-Rad, Hercules, CA, USA). Relative expression of target genes was calculated using the  $2^{-\Delta\Delta\text{Ct}}$  method by normalizing to the

housekeeping gene expression. To determine transcript levels by qPCR, the following primers were used:

<b>Primer Name</b>	<b>Sequence (5' – 3')</b>
<b>Total NEAT1_FW</b>	5' - GCCTTGTAGATGGAGCTTGC - 3'
<b>Total NEAT1_RW</b>	5' - GCACAACACAATGACACCCT - 3'
<b>TPX2_FW</b>	5' – TTCAAGGCTCGTCCAAACACCG -3'
<b>TPX2_RW</b>	5' – GCTCTCTTCTCAGTAGCCAGCT -3'
<b>GAPDH_FW</b>	5' – ACAGTCAGCCGCATCTTCTT – 3'
<b>GAPDH_RW</b>	5' – AATGAAGGGGTCATTGATGG – 3'
<b>ACTIN_FW</b>	5' - TCGGTTACACCCTTTCTTGA – 3'
<b>ACTIN_RW</b>	5' - AAAGCCATGCCAATCTCATC – 3'
<b>FOXM1_FW</b>	5' – TCTGCCAATGGCAAGGTCTCCT - 3'
<b>FOXM1_RW</b>	5' – CTGGATTCGGTCGTTTCTGCTG – 3'
<b>KIF11_FW</b>	5' – ACAGCTGACATGGATGGGAA - 3'
<b>KIF11_R</b>	5' – TCTGAAAGCTGGATGTGGGT – 3'
<b>NUF2_FW</b>	5' – CTGCTTCCAAACCATGCACT – 3'
<b>NUF2_RW</b>	5' – AAAATCCCAGCTGCACAAGG – 3'
<b>CLASP2_FW</b>	5' – CTGTTAGTGCCATGCGAGTC – 3'
<b>CLASP2_RW</b>	5' – TTCTGCCACATCTTCCGTCT – 3'
<b>AURKA_FW</b>	5' – TCCTGAGGAGGAACTGGCATCAAA – 3'
<b>AURKA_RW</b>	5' – TACCCAGAGGGCGACCAATTTCAA – 3'
<b>INCEP_FW</b>	5' - AGGCTCCTGAATGTTGAGGTGC – 3'
<b>INCEP_RW</b>	5' - GTGTGCTGTTGGCAATCTCCGT – 3'

<b>E2F1_FW</b>	5' – AGCTGGACCACCTGATGAAT – 3'
<b>E2F1_RW</b>	5' – GAGGGGCTTTGATCACCATA – 3'
<b>PRKCA_FW</b>	5' – GCCTATGGCGTCCTGTTGTATG – 3'
<b>PRKCA_RW</b>	5' – GAAACAGCCTCCTTGGACAAGG – 3'
<b>KIF23_FW</b>	5' - GTAGCAAGACCTGTAGACAAGGC – 3'
<b>KIF23_RW</b>	5' – TTCGCATGACGGCAAAGGTGGA – 3'
<b>EXO-1 FW</b>	5' – AGCTACGCTGGGCAATATGT - 3'
<b>EXO-1_RW</b>	5' – ACTTCTTGAATGGGCAGGCA – 3'
<b>FEN1_FW</b>	5' – AGTGGAGCGAGCCAAATGAA – 3'
<b>FEN1_RW</b>	5' – TACTCAGCCTCTTGACCCCA – 3'
<b>BRCA1_FW</b>	5' – GTCCCATCTGTCTGGAGTTGA – 3'
<b>BRCA1_RW</b>	5' – GGCCCTTTCTTCTGGTTGAGA – 3'
<b>HELLS_FW</b>	5' – AGCGGTTGTGAGGAGTTAGC – 3'
<b>HELLS_RW</b>	5' – CATGCCTGGACACTCACCC – 3'
<b>CDC6_FW</b>	5' – AAGCTGTCTCGGGCATTGAA – 3'
<b>CDC6_RW</b>	5' – GCTGAGAGGCAGGGCTTTTA – 3'
<b>POLD1_FW</b>	5' – AAACGCTGTTTGAAGCGGCA – 3'
<b>POLD1_RW</b>	5' – GAGGTGCATCATCATCATCCCA – 3'

### **Western blot analysis**

Cells were homogenized with PLB lysis buffer (Promega, Madison, WI, USA) supplemented with Protease Inhibitors cocktail (Bimake, Houston, TX, USA). 25-40 µg of total cell lysate were separated using SDS–PAGE using Bio-Rad apparatus (Bio-Rad, Hercules, CA, USA)

with precast Any kD Acrilamide Gels (Bio-Rad, Hercules, CA, USA), electro-transferred onto nitrocellulose membranes (Bio-Rad, Hercules, CA, USA). Membranes were blocked with 5% milk-PBST for at least 2 hours and then immunoblotted with primary antibodies overnight at 4°C in BSA 2%-PBS Tween 0.1% (PBST). Membranes were washed three times in PBST solution and then incubated with a secondary antibody diluted in milk 2% - PBST for 2 hours at room temperature. Chemiluminescence was detected using WESTAR ECL substrate for western blotting (Cyanagen) and the ChemiDoc MP System (Bio-Rad).

The experiments were repeated at least three times.

The table below reported the antibody used:

<b>Antibody</b>	<b>Company</b>	<b>Code</b>	<b>Source</b>	<b>Dilution</b>
<b>Anti-AURKA</b>	Cell signalling technology	14475	Rabbit pAb	1:1000 BSA 2%-PBST
<b>Anti-pAURKA Thr 288</b>	Cell signalling technology	3079	Rabbit pAb	1:500 BSA 2%-PBST
<b>Anti-PLK1</b>	Cell signalling technology	4513	Rabbit pAb	1:1000 BSA 2%-PBST
<b>Anti-CCNB1 (Anti-CycB1)</b>	Santa Cruz Biotechnology	sc-245	Mouse mAb	1:500 BSA 2%-PBST
<b>Anti-TPX2</b>	Cell signalling technology	12245	Rabbit pAb	1:1000 BSA 2%-PBST
<b>Anti-GAPDH</b>	Cell signalling technology	12245	Rabbit pAb	1:2000 BSA 2%-PBST
<b>Anti-ACTIN</b>	Santa Cruz Biotechnology	sc-8432	Mouse mAb	1:2000 BSA 2%-PBST
<b>Anti-mouse IgG</b>	Amersham	NXA931	HRP-linked	1:2000-1:5000 milk 2%-PBST
<b>Anti-rabbit IgG</b>	Amersham	NA934	HRP-linked	1:2000-1: 5000 milk 2%-PBST

## **Immunofluorescence**

0,15 x 10<sup>6</sup> cells for each condition were harvested, immobilized onto glass slides through Cytospin (Thermo Scientific), fixed in 4% paraformaldehyde in PBS for 7 minutes at 22°C, then washed three times with PBS. Cells were permeabilized (0.5% Triton X-100 in PBS) for 15 minutes, washed three times with PBS and blocked for 1 hour at 22°C with 1.5% BSA in PBS. After blocking, slides were washed three times in PBS and incubated for 1 hour at 22°C in the dark with Anti- $\alpha$ -Tubulin Alexa Fluor 488 (Abcam; #185031, 1:100) to stain microtubules. After three PBS washes nuclei staining was performed with DAPI (Sigma-Aldrich) and mounted under coverslips with Glycerol-PBS mounting media. Images were acquired by Leica TCS SP8 confocal laser scanning microscope (DMi8); acquisitions were performed with 63X immersion oil objectives. Conversion of imaged z-stacks into average intensity projections were processed by Leica Microsystem software (Leica Application Suite X - LAS X).

## **Sequencing and DEG analysis**

Before library preparation, RNA concentration was evaluated through Qubit™ RNA Broad Range Assay Kit (Invitrogen, Waltham, MA, USA) while RNA quality was established on 4200 TapeStation (Agilent Technologies, Santa Clara, CA, USA) using RNA Screen tape kit (Agilent Technologies, Santa Clara, CA, USA). According to the TruSeq Stranded Total RNA (San Diego, CA, USA) protocol, 500 ng of RNA for each sample with RIN value between 9 and 10, were used for RNA sequencing. Final libraries with optimal quality and quantity criteria, assessed by D1000 Screen tape kit (Agilent Technologies) and by Qubit® dsDNA High Sensitivity Assay Kit (Invitrogen). Sequencing read quality was assessed with FastQC (v.0.11.9)<sup>3</sup>. Total-RNA (stranded) sequences were aligned to the reference human genome (GRCh38) using STAR (v.2.7.9a)<sup>4</sup> in two-pass mode. Gene expression was quantified at the gene level, utilizing comprehensive annotations from Gencode (v38 GTF File). Samples were normalized and adjusted for library size using the variance stabilizing transformation in the R statistical environment via the DESeq2 (v1.28.1)<sup>5</sup> pipeline. Differential expression analysis between groups employed the embedded Independent Filtering procedure to exclude genes with low expression across most samples. Unless specified otherwise, limma (v.3.44.3) package was used for GSEA (Camera, use ranks set to FALSE), and geneset collections were obtained from the Molecular Signature Database (MSigDB)<sup>6</sup>. P-values underwent false discovery rate (FDR) correction (threshold: 0.05) for multiple testing. Data are available at ArrayExpress; access code: E-MTAB-13925.

### **Enrichment analysis**

Biological processes analyses were performed by EnrichR enrichment website tool (<https://maayanlab.cloud/Enrichr/>). Genes from differential expression analyses with a fold change  $\leq -0,7$  and  $p_{adj} \leq 0,05$  were used to identify GO and pathways ( $n = 88$ ) and were used to perform GO and pathways analyses. Enriched biological processes were considered significant by applying a threshold of 0.05 on  $p$ -value adjusted by Benjamini-Hochberg correction for multiple testing.

### **Connectivity Map**

Differential gene expression signature obtained comparing AMO-1\_NEAT1 KD and AMO-1\_SCR cells, was used as input of the Connectivity Map (cMap, v1.1.1.43, dataset v1.1.1.2, accessed via <https://clue.io>). cMAP output is list of perturbagens (pharmacological and genetic strategies - the latter not considered in this study) ranked according to the similarity between the input and the signature they induce in a set of cell lines.

Since at the time of our query, none of the cell lines present on the cMap database were of multiple myeloma cells, we used the option “summary” which, given a set of connectivity scores for a particular inhibitor, summarizes those scores across all the eight cell lines tested. Compounds presenting a similar transcriptional signature to our query were selected considering a connectivity score  $> 90$ .

### **Multi-Omics Data in CoMMpass Study**

Multi-omics data about bone marrow MM samples at baseline (BM\_1) were publicly accessible from MMRF CoMMpass Study (<https://research.themmr.org/>) including more than 1000 MM patients from several worldwide sites and retrieved from the Interim Analysis 20 (MMRF\_CoMMpass\_IA20, accessed on 19 January 2023). Transcript per Million (TPM) reads values of the AURKA transcript were retrieved using Salmon gene expression quantification data (MMRF\_CoMMpass\_IA20\_salmon\_geneUnstranded\_TPM) in 767 BM\_1 MM patients. Clinical data regarding Overall Survival (OS) and Progression free Survival (PFS) were considered in 767 MM patients for which both RNA-seq expression and survival data were available. Non-synonymous (NS) somatic mutation variants and counts data were obtained from whole exome sequencing (WES) analyses, main IgH translocations were inferred from

RNA-seq spike expression estimates of known target genes and Copy Number Alteration (CNA) data were retrieved by means of Next generation Sequencing (NGS)-based fluorescence in situ hybridization (FISH)<sup>7</sup> in 489 MM cases for which all data were available<sup>8</sup>. The presence of a specific CNA was considered when occurring in at least one of the investigated cytoband at a 20% cut-off for each considered chromosomal aberration, as previously reported<sup>7</sup>.

### **Survival analyses**

Survival analyses were performed using *survival*<sup>9,10</sup> and *survminer*<sup>11</sup> packages in R Bioconductor (version 4.1.2). Kaplan-Meier analysis was applied on OS and PFS data in patients stratified in quartiles and by comparing the first and fourth quartiles. Log-Rank test p-value was calculated to measure the global difference between survival curves. Cox proportional hazards model was applied as univariate analysis on single molecular variables, age and International Staging System (ISS) groups in relation to OS and PFS data in 489 MM cases for which all information were accessible. Cox regression multivariate analysis was applied on all significant features after BH correction. Forest plot was used to summarize Cox Proportional Hazard Model.

### **Statistical analysis**

For functional assays statistical analysis was performed using GraphPad Prism Software (version 9.5.1 for Windows, GraphPad Software, San Diego, CA, USA). Statistical significance was determined using the Student's *t*-test. Differences were considered significant when *P* values were \**P*<0.05, \*\**P*<0.01 or \*\*\**P*<0.001.

### **Supplementary methods references**

1. Riccardi, C. and Nicoletti, I. (2006) Analysis of Apoptosis by Propidium Iodide Staining and Flow Cytometry. <http://www.natureprotocols.com>.
2. Mereu E, Abbo D, Paradzik T, Cumerlato M, Bandini C, Labrador M, Maccagno M, Ronchetti D, Manicardi V, Neri A, et al. Euchromatic Histone Lysine Methyltransferase 2 Inhibition Enhances Carfilzomib Sensitivity and Overcomes Drug Resistance in Multiple Myeloma Cell Lines. *Cancers*. 2023; 15(8):2199.
3. Andrews, S. Babraham Bioinformatics - FastQC A Quality Control tool for High Throughput Sequence Data. <https://www.bioinformatics.babraham.ac.uk/projects/fastqc/> (2010).

4. Dobin, A. *et al.* STAR: ultrafast universal RNA-seq aligner. *Bioinformatics* **29**, 15–21 (2013).
5. Love, M. I., Huber, W. & Anders, S. Moderated estimation of fold change and dispersion for RNA-seq data with DESeq2. *Genome Biology* **15**, 550 (2014).
6. Liberzon, A. *et al.* The Molecular Signatures Database (MSigDB) hallmark gene set collection. *Cell Syst* **1**, 417–425 (2015).
7. Miller, C. *et al.* A comparison of clinical FISH and sequencing based FISH estimates in multiple myeloma: An MMRF CoMMpass analysis. In: Hematology TAsO, editor. The American Society of Hematology; 2016: Blood; 2016. p. 374.
8. Todoerti K, Ronchetti D, Favasuli V, Maura F, Morabito F, Bolli N, Taiana E, Neri A. DIS3 mutations in multiple myeloma impact the transcriptional signature and clinical outcome. *Haematologica*. 2021.
9. Therneau T (2021). A Package for Survival Analysis in R. R package version 3.2-11, <URL: <https://CRAN.R-project.org/package=survival>>.
10. Terry M. Therneau, Patricia M. Grambsch (2000). *Modeling Survival Data: Extending the Cox Model*. Springer, New York. ISBN 0-387-98784-3.
11. Alboukadel Kassambara, Marcin Kosinski and Przemyslaw Biecek (2021). *survminer: Drawing Survival Curves using ‘ggplot2’*. R package version 0.4.9. <https://CRAN.R-project.org/package=survminer>.

**Supplementary table 1**

<b>Cat n°</b>	<b>Drug</b>	<b>Target</b>	<b>Pathway</b>
S2698	RS-127445	5-HT Receptor	Neuronal Signaling
S2894	SB742457	5-HT Receptor	Neuronal Signaling
S1549	Nebivolol HCl	Adrenergic Receptor	Neuronal Signaling
S8114	ICI-118551 Hydrochloride	Adrenergic Receptor	GPCR & G Protein
S1078	MK-2206 2HCl	Akt	PI3K/Akt/mTOR
S2808	Ipatasertib (GDC-0068)	Akt	PI3K/Akt/mTOR
S4854	Bedaquiline fumarate	Anti-infection	Microbiology
S1188	Anastrozole	Aromatase	Endocrinology & Hormones
S8292	Selonsertib (GS-4997)	ASK	Apoptosis
S1092	KU-55933 (ATM Kinase Inhibitor)	ATM/ATR	DNA Damage
S1570	KU-60019	ATM/ATR	DNA Damage
S7102	VE-822	ATM/ATR	PI3K/Akt/mTOR
S8556	AZ31	ATM/ATR	DNA Damage
S8666	BAY 1895344 (BAY-1895344)	ATM/ATR	DNA Damage
S8680	AZD1390	ATM/ATR	PI3K/Akt/mTOR
S1048	Tozasertib (VX-680, MK-0457)	Aurora Kinase	Cell Cycle
S1133	Alisertib (MLN8237)	Aurora Kinase	Cell Cycle
S1147	Barasertib (AZD1152-HQPA)	Aurora Kinase	Cell Cycle
S1451	Aurora A Inhibitor I	Aurora Kinase	Cell Cycle
S2740	GSK1070916	Aurora Kinase	Cell Cycle
S2770	MK-5108 (VX-689)	Aurora Kinase	Cell Cycle
S7065	MK-8745	Aurora Kinase	Cell Cycle
S2744	CCT137690	Aurora Kinase	Cell Cycle
S1023	Erlotinib HCl (OSI-744)	Autophagy,EGFR	Protein Tyrosine Kinase
S1049	Y-27632 2HCl	Autophagy,ROCK	Cell Cycle
S7849	BDA-366	Bcl-2	Apoptosis
S8048	Venetoclax (ABT-199, GDC-0199)	Bcl-2	Apoptosis
S7790	A-1210477	Bcl-2	Apoptosis
S8591	FX1	Bcl-6	Apoptosis
S2899	GNF-2	Bcr-Abl	Angiogenesis
S2680	Ibrutinib (PCI-32765)	BTK	Angiogenesis
S7173	Spebrutinib (CC-292, AVL-292)	BTK	Angiogenesis
S7257	CNX-774	BTK	Angiogenesis
S7734	LFM-A13	BTK	Angiogenesis
S8777	Evobrutinib	BTK	Protein Tyrosine Kinase
S1094	PF-04217903	c-Met	Protein Tyrosine Kinase

S1114	JNJ-38877605	c-Met	Protein Tyrosine Kinase
S2747	AMG-458	c-Met	Protein Tyrosine Kinase
S2753	Tivantinib (ARQ 197)	c-Met	Protein Tyrosine Kinase
S2761	NVP-BVU972	c-Met	Protein Tyrosine Kinase
S7067	Tepotinib (EMD 1214063)	c-Met	Protein Tyrosine Kinase
S7674	Savolitinib(AZD6094, HMPL-504)	c-Met	Protein Tyrosine Kinase
S8167	AMG 337	c-Met	Protein Tyrosine Kinase
S7564	SAR125844	c-Met	Protein Tyrosine Kinase
S1112	SGX-523	c-Met	Protein Tyrosine Kinase
S2788	Capmatinib (INCB28060)	c-Met	Protein Tyrosine Kinase
S7436	NH125	CaMK	Neuronal Signaling
S7499	ESI-09	cAMP	GPCR & G Protein
S7500	HJC0350	cAMP	GPCR & G Protein
S8012	Otenabant (CP-945598) HCl	Cannabinoid Receptor	GPCR & G Protein
S7461	LDC000067	CDK	Cell Cycle
S7992	LDC4297 (LDC044297)	CDK	Cell Cycle
S8652	Skp2 inhibitor C1 (SKPin C1)	CDK	Cell Cycle
S8727	Atuveciclib (BAY-1143572)	CDK	Cell Cycle
S1116	Palbociclib (PD-0332991) HCl	CDK	Cell Cycle
S1579	Palbociclib (PD0332991) Isethionate	CDK	Cell Cycle
S2626	Rabusertib (LY2603618)	Chk	Cell Cycle
S2683	CHIR-124	Chk	Cell Cycle
S8253	CCT245737	Chk	Cell Cycle
S8632	Chk2 Inhibitor II (BML-277)	Chk	Cell Cycle
S2903	Lumiracoxib	COX	Neuronal Signaling
S4136	Carprofen	COX	Neuronal Signaling
S7725	BLZ945	CSF-1R	Protein Tyrosine Kinase
S8042	GW2580	CSF-1R	Protein Tyrosine Kinase
S7651	SB225002	CXCR	GPCR & G Protein
S8813	LIT-927	CXCR	Immunology & Inflammation
S1115	Odanacatib (MK-0822)	Cysteine Protease	Proteases
S7241	AGI-6780	Dehydrogenase	Metabolism
S8619	NCT-503	Dehydrogenase	Metabolism
S2868	Alogliptin (SYK-322) benzoate	DPP-4	Proteases
S3031	Linagliptin	DPP-4	Proteases

S4002	Sitagliptin phosphate monohydrate	DPP-4	Proteases
S4697	Saxagliptin hydrate	DPP-4	Proteases
S5063	Trelagliptin succinate	DPP-4	Proteases
S5079	Sitagliptin	DPP-4	Proteases
S5365	Alogliptin	DPP-4	Proteases
S5909	Anagliptin	DPP-4	Proteases
S7513	Trelagliptin	DPP-4	Proteases
S8565	Omarigliptin (MK-3102)	DPP-4	Proteases
S7140	TCID	DUB	Ubiquitin
S8047	Dynasore	Dynamamin	Cytoskeletal Signaling
S7129	PYR-41	E1 Activating	Ubiquitin
S1173	WZ4002	EGFR	Protein Tyrosine Kinase
S2185	AST-1306	EGFR	Protein Tyrosine Kinase
S7206	CNX-2006	EGFR	Protein Tyrosine Kinase
S7786	Erlotinib	EGFR	Protein Tyrosine Kinase
S8724	Lazertinib (YH25448,GNS-1480)	EGFR	Protein Tyrosine Kinase
S1167	CP-724714	EGFR,HER2	Protein Tyrosine Kinase
S2192	Sapitinib (AZD8931)	EGFR,HER2	Protein Tyrosine Kinase
S1456	Zibotentan (ZD4054)	Endothelin Receptor	GPCR & G Protein
S2097	Ambrisentan	Endothelin Receptor	GPCR & G Protein
S5916	GSK 5959	Epigenetic Reader Do	Epigenetics
S8296	dBET1	Epigenetic Reader Do	Epigenetics
S1216	PFI-1 (PF-6405761)	Epigenetic Reader Domain	Epigenetics
S7110	(+)-JQ1	Epigenetic Reader Domain	Epigenetics
S7620	GSK1324726A (I-BET726)	Epigenetic Reader Domain	Epigenetics
S7835	I-BRD9	Epigenetic Reader Domain	Epigenetics
S7906	PFI-4	Epigenetic Reader Domain	Epigenetics
S8180	PF-CBP1 HCl	Epigenetic Reader Domain	Epigenetics
S8190	CPI-637	Epigenetic Reader Domain	Epigenetics
S8265	GSK6853	Epigenetic Reader Domain	Epigenetics
S7525	XMD8-92	ERK	MAPK
S7709	VX-11e	ERK	MAPK
S8534	LY3214996	ERK	MAPK
S2631	URB597	FAAH	Metabolism
S2666	PF-3845	FAAH	Metabolism
S2828	JNJ-1661010	FAAH	Metabolism
S1593	Apixaban	Factor Xa	Metabolism
S3002	Rivaroxaban	Factor Xa	Metabolism

S7167	SSR128129E	FGFR	Angiogenesis
S8493	PD-166866 (PD166866)	FGFR	Angiogenesis
S8503	BLU-554 (BLU554)	FGFR	Angiogenesis
S8675	H3B-6527	FGFR	Protein Tyrosine Kinase
S8548	FGF401	FGFR	Protein Tyrosine Kinase
S8023	TCS 359	FLT3	Angiogenesis
S2861	CTEP (RO4956371)	GluR	Neuronal Signaling
S2251	(-)-Huperzine A (HupA)	GluR,AChR	Neuronal Signaling
S8452	BAY-876	GLUT	Metabolism
S7753	BPTES	Glutaminase	Proteases
S7263	AZD1981	GPR	Endocrinology & Hormones
S1263	CHIR-99021 (CT99021)	GSK-3	PI3K/Akt/mTOR
S2729	SB415286	GSK-3	PI3K/Akt/mTOR
S2745	CHIR-98014	GSK-3	PI3K/Akt/mTOR
S2924	CHIR-99021 (CT99021) HCl	GSK-3	PI3K/Akt/mTOR
S7063	LY2090314	GSK-3	PI3K/Akt/mTOR
S7193	1-Azakenpaullone	GSK-3	PI3K/Akt/mTOR
S7435	AR-A014418	GSK-3	PI3K/Akt/mTOR
S7915	BIO-acetoxime	GSK-3	PI3K/Akt/mTOR
S4935	Asunaprevir	HCV Protease	Proteases
S5402	Dasabuvir(ABT-333)	HCV Protease	Proteases
S2012	PCI-34051	HDAC	Epigenetics
S7229	RGFP966	HDAC	Epigenetics
S7473	Nexturastat A	HDAC	DNA Damage
S7595	Santacruzamate A (CAY10683)	HDAC	DNA Damage
S7596	CAY10603	HDAC	DNA Damage
S2216	Mubritinib (TAK 165)	HER2	Protein Tyrosine Kinase
S2816	Tyrphostin AG 879	HER2	Protein Tyrosine Kinase
S8362	Irbinitinib (ARRY-380, ONT-380)	HER2	Protein Tyrosine Kinase
S2919	IOX2	HIF	Angiogenesis
S2905	JNJ-7777120	Histamine Receptor	Neuronal Signaling
S5926	Pitolisant hydrochloride	Histamine Receptor	Neuronal Signaling
S8776	WM-1119	Histone Acetyltransf	Epigenetics
S4800	Daminozide	Histone Demethylase	Epigenetics
S7574	GSK-LSD1 2HCl	Histone Demethylase	Epigenetics
S7680	SP2509	Histone Demethylase	Epigenetics
S7795	ORY-1001 (RG-6016) 2HCl	Histone Demethylase	Epigenetics
S7079	SGC 0946	Histone Methyltransferase	Epigenetics
S7165	UNC1999	Histone Methyltransferase	Epigenetics
S7230	UNC0642	Histone Methyltransferase	Epigenetics

S7294	PFI-2 HCl	Histone Methyltransferase	Epigenetics
S7572	A-366	Histone Methyltransferase	Epigenetics
S7575	LLY-507	Histone Methyltransferase	Epigenetics
S7656	CPI-360	Histone Methyltransferase	Epigenetics
S7748	EPZ015666(GSK3235025)	Histone Methyltransferase	Epigenetics
S7820	EPZ020411 2HCl	Histone Methyltransferase	Epigenetics
S7983	A-196	Histone Methyltransferase	Epigenetics
S8340	SGC2085	Histone Methyltransferase	Epigenetics
S8479	LLY-283	Histone Methyltransferase	Epigenetics
S7004	EPZ005687	Histone Methyltransferase	Epigenetics
S7061	GSK126	Histone Methyltransferase	Epigenetics
S7128	Tazemetostat (EPZ-6438)	Histone Methyltransferase	Epigenetics
S7282	NMS-E973	HSP (e.g. HSP90)	Cytoskeletal Signaling
S7751	VER155008	HSP (e.g. HSP90)	Cytoskeletal Signaling
S2695	Nepicastat (SYN-117) HCl	Hydroxylase	Metabolism
S4926	(R)-Nepicastat HCl	Hydroxylase	Metabolism
S8657	PF-06840003	IDO	Metabolism
S1093	GSK1904529A	IGF-1R	Protein Tyrosine Kinase
S7668	Picropodophyllin (PPP)	IGF-1R	Protein Tyrosine Kinase
S8660	GI254023X	Immunology & Inflammation related	Immunology & Inflammation
S7809	MCC950(CP-456773)	Immunology & Inflammation related	Immunology & Inflammation
S2005	Raltegravir (MK-0518)	Integrase	Microbiology
S5245	Raltegravir potassium	Integrase,HIV Protease	Microbiology
S4907	SC-514	IκB/IKK	NF-κB
S8044	BMS-345541	IκB/IKK	NF-κB
S5903	JANEX-1	JAK	JAK/STAT
S8538	PF-06651600	JAK	JAK/STAT
S8541	FM-381	JAK	JAK/STAT
S7508	JNK Inhibitor IX	JNK	MAPK
S8201	BI-78D3	JNK	MAPK
S1452	Ispinesib (SB-715992)	Kinesin	Cytoskeletal Signaling
S2182	SB743921 HCl	Kinesin	Cytoskeletal Signaling
S5933	K 858	Kinesin	Cytoskeletal Signaling
S4904	JZL184	Lipase	Metabolism
S7364	Atglistatin	Lipase	Metabolism
S7457	XEN445	Lipase	Metabolism
S1472	Safinamide Mesylate	MAO	Metabolism
S7875	NVP-CGM097	Mdm2	Apoptosis
S1008	Selumetinib (AZD6244)	MEK	MAPK
S1020	PD184352 (CI-1040)	MEK	MAPK
S1036	PD0325901	MEK	MAPK

S1066	SL-327	MEK	MAPK
S1089	Refametinib (RDEA119, Bay 86-9766)	MEK	MAPK
S1102	U0126-EtOH	MEK	MAPK
S1475	Pimasertib (AS-703026)	MEK	MAPK
S2673	Trametinib (GSK1120212)	MEK	MAPK
S8041	Cobimetinib (GDC-0973, RG7420)	MEK	MAPK
S7430	SB-3CT	MMP	Proteases
S7421	CGP 57380	MNK	MAPK
S7632	TH588	MTH1	DNA Damage
S1226	KU-0063794	mTOR	PI3K/Akt/mTOR
S1266	WYE-354	mTOR	PI3K/Akt/mTOR
S1555	AZD8055	mTOR	PI3K/Akt/mTOR
S2624	OSI-027	mTOR	PI3K/Akt/mTOR
S2689	WAY-600	mTOR	PI3K/Akt/mTOR
S2783	Vistusertib (AZD2014)	mTOR	PI3K/Akt/mTOR
S2811	Sapanisertib (INK 128, MLN0128)	mTOR	PI3K/Akt/mTOR
S7035	XL388	mTOR	PI3K/Akt/mTOR
S7886	CC-223	mTOR	PI3K/Akt/mTOR
S8040	GDC-0349	mTOR	PI3K/Akt/mTOR
S8642	GSK'963	NF-κB, TNF-alpha	NF-κB
S5476	Rolapitant	NK1-receptor	GPCR
S5696	JNJ0966	Others	Others
S7213	Thiamet G	Others	Others
S7270	SRPIN340	Others	Others
S7272	4μ8C	Others	Others
S9360	4-Hydroxyquinazoline	Others	antiplatelet
S1195	TAK-700 (Orteronel)	P450 (e.g. CYP17)	Metabolism
S2921	PF-4981517	P450 (e.g. CYP17)	Metabolism
S3673	Sulfaphenazole	P450 (e.g. CYP17)	Metabolism
S7093	IPA-3	PAK	Cytoskeletal Signaling
S1004	Veliparib (ABT-888)	PARP	DNA Damage
S1060	Olaparib (AZD2281, KU-0059436)	PARP	DNA Damage
S2741	Niraparib (MK-4827)	PARP	DNA Damage
S7238	NVP-TNKS656	PARP	DNA Damage
S8363	NMS-P118	PARP	DNA Damage
S8592	Pamiparib (BGB-290)	PARP	DNA Damage
S1512	Tadalafil	PDE	Metabolism
S1550	Pimobendan	PDE	Metabolism
S2312	Icariin	PDE	Metabolism
S2687	Mardepodect (PF-2545920)	PDE	Metabolism
S4019	Avanafil	PDE	Metabolism

S5837	BRL-50481	PDE	Metabolism
S2620	GSK256066	PDE	Metabolism
S1536	CP-673451	PDGFR	Protein Tyrosine Kinase
S7087	GSK2334470	PDK	PI3K/Akt/mTOR
S7033	GSK2656157	PERK	Apoptosis
S7307	GSK2606414	PERK	Apoptosis
S7400	ISRIB (trans-isomer)	PERK	Apoptosis
S8278	SHP099 dihydrochloride	phosphatase	Others
S2717	CP-91149	Phosphorylase	Metabolism
S1169	TGX-221	PI3K	PI3K/Akt/mTOR
S1352	TG100-115	PI3K	PI3K/Akt/mTOR
S2636	A66	PI3K	PI3K/Akt/mTOR
S5818	acalisib (GS-9820)	PI3K	PI3K/Akt/mTOR
S7335	IPI-3063	PI3K	PI3K/Akt/mTOR
S7938	GSK2292767	PI3K	PI3K/Akt/mTOR
S7980	VPS34-IN1	PI3K	PI3K/Akt/mTOR
S8330	IPI-549	PI3K	PI3K/Akt/mTOR
S8456	VPS34 inhibitor 1 (Compound 19, PIK-III analogue)	PI3K	PI3K/Akt/mTOR
S8581	Serabelisib (INK-1117,MLN-1117,TAK-117)	PI3K	PI3K/Akt/mTOR
S8672	Tenalisib (RP6530)	PI3K	PI3K/Akt/mTOR
S8005	SMI-4a	Pim	JAK/STAT
S7208	Bisindolylmaleimide I (GF109203X)	PKC	TGF-beta/Smad
S1109	BI 2536	PLK	Cell Cycle
S2193	GSK461364	PLK	Cell Cycle
S7248	Ro3280	PLK	Cell Cycle
S7255	NMS-P937 (NMS1286937)	PLK	Cell Cycle
S7720	SBE 13 HCl	PLK	Cell Cycle
S2871	T0070907	PPAR	DNA Damage
S7767	AZ6102	PPAR	DNA Damage
S2224	UK 383367	Procollagen C Proteinase	Metabolism
S7462	PI-1840	Proteasome	Proteases
S8651	bpV (HOpic)	PTEN	Others
S3057	Azilsartan Medoxomil	RAAS	Endocrinology & Hormones
S4102	Eprosartan Mesylate	RAAS	Endocrinology & Hormones
S5069	Dabrafenib Mesylate	Raf	MAPK
S7964	PLX7904	Raf	MAPK
S8745	LXH254	Raf	MAPK
S8031	NSC 23766	Rho	Cell Cycle
S1474	GSK429286A	ROCK	Cell Cycle
S8489	GSK180736A (GSK180736)	ROCK	Cell Cycle

S7176	SKI II	S1P Receptor	GPCR & G Protein
S7177	PF-543	S1P Receptor	GPCR & G Protein
S7218	Alvelestat (AZD9668)	Serine Protease	Proteases
S8457	UK-371804 HCl	Serine Protease	Proteases
S8465	GSK'872 (GSK2399872A)	Serine/threonin kinase	Apoptosis
S7188	CID755673	Serine/threonin kinase, CaMK	Apoptosis
S1548	Dapagliflozin	SGLT	GPCR & G Protein
S2760	Canagliflozin	SGLT	GPCR & G Protein
S5566	Dapagliflozin propanediol monohydrate	SGLT	GPCR & G Protein
S5901	Canagliflozin hemihydrate	SGLT	GPCR & G Protein
S8022	Empagliflozin (BI 10773)	SGLT	GPCR & G Protein
S8558	Tofogliflozin (CSG 452)	SGLT	GPCR & G Protein
S8637	Ipragliflozin (ASP1941)	SGLT	GPCR & G Protein
S5413	Ertugliflozin	SGLT2	Ion-Channel
S1541	Selisistat (EX 527)	Sirtuin	Epigenetics
S2804	Sirtinol	Sirtuin	Epigenetics
S7845	SirReal2	Sirtuin	Epigenetics
S8245	Thiomyristoyl	Sirtuin	DNA Damage
S2785	A-803467	Sodium Channel	Transmembrane Transporters
S2285	Cryptotanshinone	STAT	JAK/STAT
S7024	Stattic	STAT	JAK/STAT
S7501	HO-3867	STAT	JAK/STAT
S1189	Aprepitant	Substance P	Others
S7006	BAY-61-3606	Syk	Angiogenesis
S1186	BIBR 1532	Telomerase	DNA Damage
S1067	SB431542	TGF-beta/Smad	TGF-beta/Smad
S7146	DMH1	TGF-beta/Smad	TGF-beta/Smad
S7624	SD-208	TGF-beta/Smad	TGF-beta/Smad
S7959	SIS3 HCl	TGF-beta/Smad	TGF-beta/Smad
S7507	LDN-193189 2HCl	TGF-beta/Smad	TGF-beta/Smad
S7148	ML347	TGF-beta/Smad, ALK	TGF-beta/Smad
S5074	Argatroban Monohydrate	Thrombin	Others
S1577	Tie2 kinase inhibitor	Tie-2	Protein Tyrosine Kinase
S8677	Cu-CPT22	TLR	Immunology & Inflammation
S8641	Nec-1s (7-Cl-O-Nec1)	TNF-alpha	Apoptosis
S8787	GSK'547	TNF-alpha	Apoptosis
S7465	FTI 277 HCl	Transferase	Metabolism
S2891	GW441756	Trk receptor	Protein Tyrosine Kinase
S7960	Larotrectinib (LOXO-101) sulfate	Trk receptor	Protein Tyrosine Kinase

S2773	SB705498	TRPV	Others
S8238	SB366791	TRPV	Transmembrane Transporters
S5623	Bedaquiline	tuberculosis	Immunology
S2896	ZM 323881 HCl	VEGFR	Protein Tyrosine Kinase
S5667	Fruquintinib	VEGFRs	VEGFR
S9500	Valbenazine tosylate	VMAT2	Others
S1525	Adavosertib (MK-1775)	Wee1	Cell Cycle
S2662	ICG-001	Wnt/beta-catenin	Stem Cells & Wnt
S8327	KYA1797K	Wnt/beta-catenin	Stem Cells & Wnt
S8644	GNF-6231	Wnt/beta-catenin	Stem Cells & Wnt

**Supplementary table 1.** List of drugs used for the high-throughput screening.

## Supplementary table 2

		IC 50 (72 hours)
Aisertib	AMO-1	32 nM
	NCI-H929	18 nM
	MM1.S	10 nM

		IC 50 (72 hours)
AURKAI-I	AMO-1	0,28 µM
	NCI-H929	0,2 µM
	MM1.S	0,11 µM

**Supplementary table 2.** IC50 calculation at 72 hours of Aisertib and AURKAI for AMO-1, NCI-H929 and MM1.S cell lines.

## Supplementary table 3

Gene ID	Gene name	Gene type	Fold change	p adj value
ENSG00000174442	ZWILCH	protein coding	-2,33	4,14E-132
ENSG00000138160	KIF11	protein coding	-1,54	2,07E-66
ENSG00000163539	CLASP2	protein coding	-1,21	8,12E-106
ENSG00000143228	NUF2	protein coding	-1,11	2,38E-32
ENSG00000161888	SPC24	protein coding	-1,01	2,18E-42
ENSG00000088325	TPX2	protein coding	-0,96	1,05E-74
ENSG00000123219	CENPK	protein coding	-0,94	6,13E-14
ENSG00000117724	CENPF	protein coding	-0,93	6,36E-39
ENSG00000152253	SPC25	protein coding	-0,92	8,91E-14
ENSG00000126787	DLGAP5	protein coding	-0,92	9,11E-26
ENSG00000102384	CENPI	protein coding	-0,92	1,61E-22
ENSG00000112029	FBXO5	protein coding	-0,88	8,72E-26
ENSG00000156970	BUB1B	protein coding	-0,87	2,03E-42
ENSG00000142945	KIF2C	protein coding	-0,86	1,03E-49
ENSG00000112742	TTK	protein coding	-0,85	3,44E-18
ENSG00000118193	KIF14	protein coding	-0,83	1,15E-22
ENSG00000129810	SGO1	protein coding	-0,81	2,27E-18
ENSG00000121152	NCAPH	protein coding	-0,81	1,50E-33
ENSG00000101639	CEP192	protein coding	-0,81	3,96E-39
ENSG00000138778	CENPE	protein coding	-0,80	4,36E-07
ENSG00000237649	KIFC1	protein coding	-0,80	3,27E-33
ENSG00000076382	SPAG5	protein coding	-0,79	3,17E-38
ENSG00000164109	MAD2L1	protein coding	-0,79	2,56E-14
ENSG00000109805	NCAPG	protein coding	-0,79	3,01E-21
ENSG00000138180	CEP55	protein coding	-0,77	1,17E-24
ENSG00000071539	TRIP13	protein coding	-0,76	4,53E-41
ENSG00000136824	SMC2	protein coding	-0,76	1,28E-19
ENSG00000121621	KIF18A	protein coding	-0,75	3,56E-15
ENSG00000184445	KNTC1	protein coding	-0,74	2,24E-24
ENSG00000113810	SMC4	protein coding	-0,71	6,56E-17

**Supplementary table 3.** List of top-thirty significant down-regulated genes belonging to mitotic spindle and microtubule organization (GO:0007052; GO:1902850) in AMO-1 NEAT1 KD cells compared to the scramble condition. Down-regulated genes are ordered according to the fold change.

## Supplementary table 4

IgH trx (RNA-seq)	N (%)
t(11;14)/CCND1	136 (20.6%)
t(6;14)/CCND3	9 (1.4%)
t(4;14)/WHSC1/FGFR3	89 (13.5%)
t(14;16)/MAF;t(14;20)/MAFB; t(8;16)/MAFA	42 (6.4%)
t(8;14)/MYC	27 (4.1%)
CNA (FISH-WES)	N (%)
del(13)(q14)/(q34)/RB1_20%	346 (52.4%)
1q21 gain_20%	240 (36.4%)
del(1)(p22)/CDKN2C_20%	199 (30.2%)
del(17)(p13)/TP53_20%	74 (11.2%)
HD	375 (56.8%)
NS Somatic Mutation (WES)	N (%)
<i>DIS3</i>	71 (10.8%)
<i>N-RAS</i>	146 (22.1%)
<i>H-RAS</i>	0 (0%)
<i>K-RAS</i>	160 (24.2%)
<i>BRAF</i>	51 (7.7%)
<i>TP53</i>	30 (4.5%)
<i>FAM46C</i>	66 (10%)
<i>TRAF3</i>	50 (7.6%)

**Supplementary Table 4.** Number and relative frequency of main IgH translocations (trx), copy number alterations (CNAs) and non-synonymous (NS) somatic mutations, in 660 BM-1 MM cases of MMRF\_CoMMpass\_IA20 cohort with available data about AURKA expression by RNA sequencing (RNA -seq), IgH trx by RNA-seq, NS somatic mutations by Whole Exome sequencing (WES) and CNAs by next generation sequencing (NGS)-based FISH (FISH-WES).

## Supplementary table 5

**A**

Variable	N (%)	OS Univariate Cox Analysis		
		HR (95% CI)	P-value	Adj. P-value
high AURKA	247 (50)	1.54 (1.11-2.13)	0.0102	<b>0.0306*</b>
Age (≥ 65 yrs)	206 (41)	2.12 (1.46-3.08)	0.0000868	<b>0.0005***</b>
ISS I	187 (38)	0.31 (0.19-0.50)	0.00000186	<b>0.0000195****</b>
ISS II	171 (34)	1.13 (0.78-1.64)	0.524	0.687
ISS III	139 (28)	2.45 (1.70-3.53)	0.00000162	<b>0.0000195****</b>
del(1p)/CDKN2C	143 (29)	1.61 (1.10-2.35)	0.0148	<b>0.0347*</b>
del(13q)/RB1	258 (52)	2.11 (1.44-3.09)	0.000119	<b>0.0005***</b>
HD	281 (56)	0.64 (0.44-0.92)	0.0149	<b>0.0347*</b>
TP53.alterations	40 (8)	1.05 (0.53-2.07)	0.892	0.892
1q21 gain/amp	164 (33)	1.68 (1.17-2.43)	0.0051	<b>0.0178*</b>
TP53.alterations + 1q21 gain/amp	19 (4)	3.63 (1.89-6.97)	0.000103	<b>0.0005***</b>
DIS3 mut	50 (10)	1.63 (1.06-2.50)	0.0264	0.052
N-RAS mut	117 (23)	0.90 (0.62-1.32)	0.596	0.732
K-RAS mut	121 (24)	1.07 (0.77-1.49)	0.694	0.762
BRAF mut	36 (7)	1.18 (0.60-2.31)	0.628	0.732
FAM46C mut	49 (10)	0.78 (0.42-1.43)	0.419	0.586
TRAF3 mut	38 (7)	0.42 (0.17-1.06)	0.0668	0.107
t(11;14)	102 (20)	0.92 (0.58-1.46)	0.726	0.762
t(4;14)	69 (14)	1.63 (1.04-2.55)	0.0335	0.058
MAF.trx	33 (7)	1.96 (1.08-3.57)	0.0276	0.052
MYC.trx	20 (4)	1.92 (0.94-3.94)	0.0748	0.112

**B**

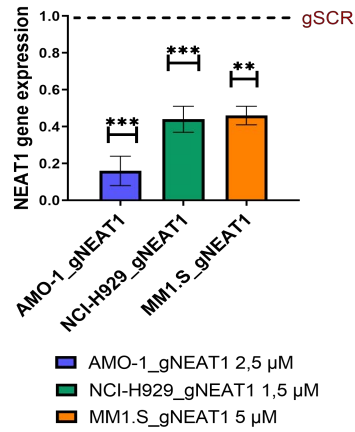
Variable	N (%)	OS Univariate Cox Analysis		
		HR (95% CI)	P-value	Adj. P-value
high AURKA	247 (50)	1.54 (1.11-2.13)	0.0102	<b>0.0306*</b>
Age (≥ 65 yrs)	206 (41)	2.12 (1.46-3.08)	0.0000868	<b>0.0005***</b>
ISS I	187 (38)	0.31 (0.19-0.50)	0.00000186	<b>0.0000195****</b>
ISS II	171 (34)	1.13 (0.78-1.64)	0.524	0.687
ISS III	139 (28)	2.45 (1.70-3.53)	0.00000162	<b>0.0000195****</b>
del(1p)/CDKN2C	143 (29)	1.61 (1.10-2.35)	0.0148	<b>0.0347*</b>
del(13q)/RB1	258 (52)	2.11 (1.44-3.09)	0.000119	<b>0.0005***</b>
HD	281 (56)	0.64 (0.44-0.92)	0.0149	<b>0.0347*</b>
TP53.alterations	40 (8)	1.05 (0.53-2.07)	0.892	0.892
1q21 gain/amp	164 (33)	1.68 (1.17-2.43)	0.0051	<b>0.0178*</b>
TP53.alterations + 1q21 gain/amp	19 (4)	3.63 (1.89-6.97)	0.000103	<b>0.0005***</b>
DIS3 mut	50 (10)	1.63 (1.06-2.50)	0.0264	0.052
N-RAS mut	117 (23)	0.90 (0.62-1.32)	0.596	0.732
K-RAS mut	121 (24)	1.07 (0.77-1.49)	0.694	0.762
BRAF mut	36 (7)	1.18 (0.60-2.31)	0.628	0.732
FAM46C mut	49 (10)	0.78 (0.42-1.43)	0.419	0.586
TRAF3 mut	38 (7)	0.42 (0.17-1.06)	0.0668	0.107
t(11;14)	102 (20)	0.92 (0.58-1.46)	0.726	0.762
t(4;14)	69 (14)	1.63 (1.04-2.55)	0.0335	0.058
MAF.trx	33 (7)	1.96 (1.08-3.57)	0.0276	0.052
MYC.trx	20 (4)	1.92 (0.94-3.94)	0.0748	0.112

**Supplementary table 5.** Results of Cox regression univariate analysis using OS (**A**) or PFS (**B**) data on AURKA expression groups, age equal to or greater than 65 years, ISS subgroups and main molecular alterations in 489 BM-1 MM cases for which all data were available. Number (N) of positive cases is indicated for each variable. Hazard Ratio, 95% Confidence Interval and Log-rank p-value are reported for each variable. In red bold are depicted all significant variables after BH correction.

\* $\leq 0.05$ ; \*\* $\leq 0.01$ ; \*\*\* $\leq 0.001$ ; \*\*\*\* $\leq 0.0001$

# Supplementary materials

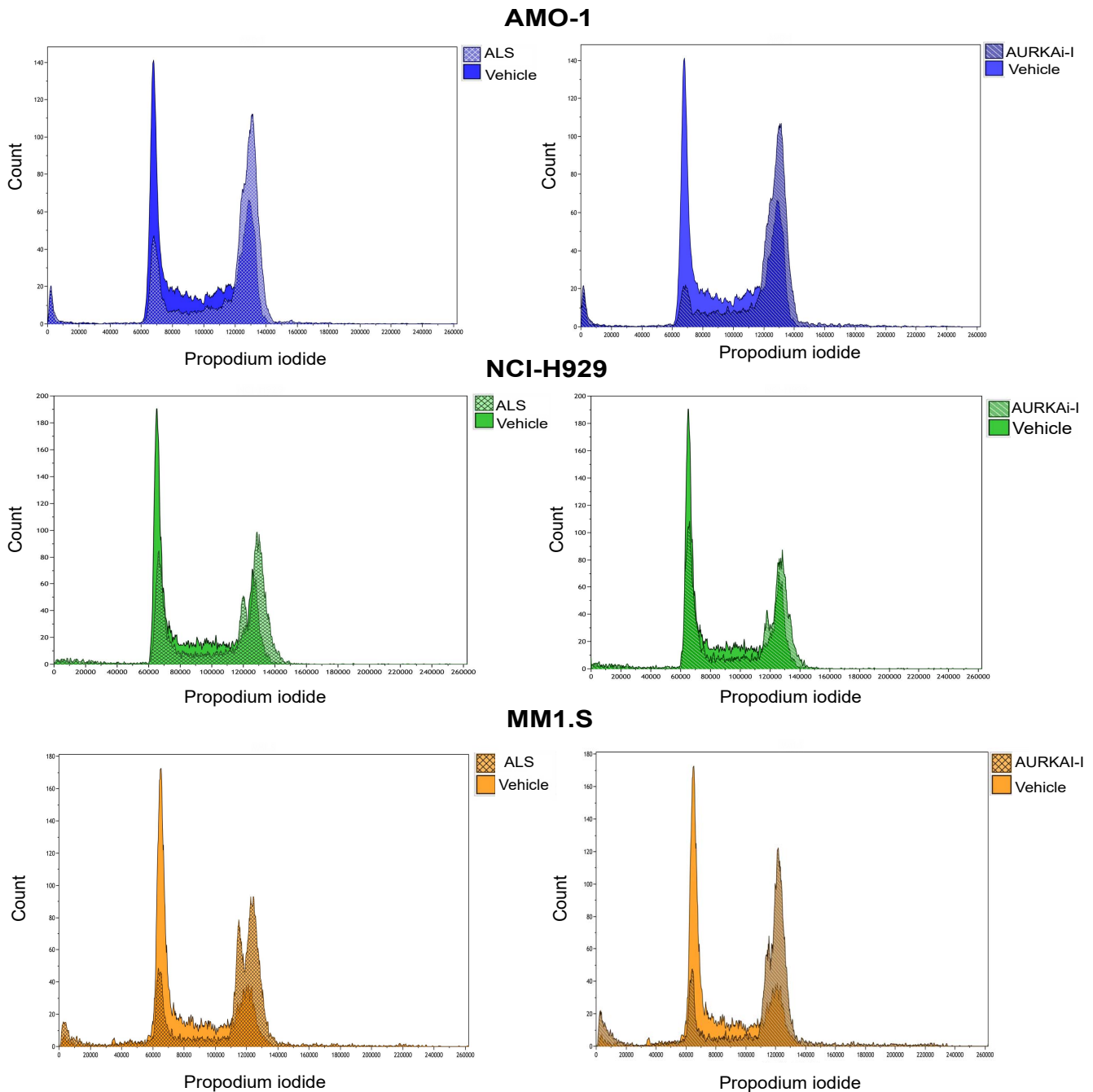
**S.1**



**Supplementary figure 1 (S.1). NEAT1 silencing in MM cells.** Quantitative real-time PCR of NEAT1 in AMO-1, NCI-H929 and MM1.S after NEAT1 KD (gNEAT1), compared to the scramble condition (96 hours of gapmeR delivery). NEAT1 expression was expressed as  $2^{-\Delta\Delta C_t}$  relative to the scramble gapmer (gSCR) at the same timepoint (n = 3).

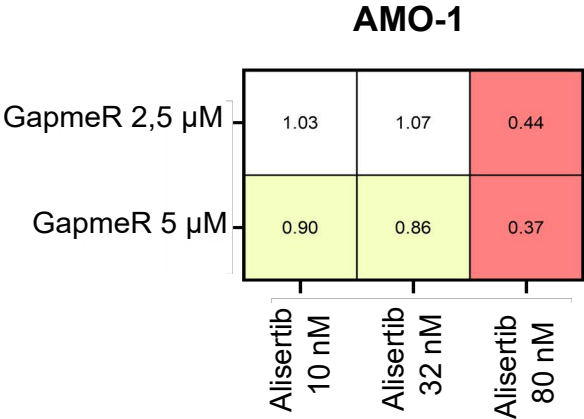
**S.2A**

**S.2B**

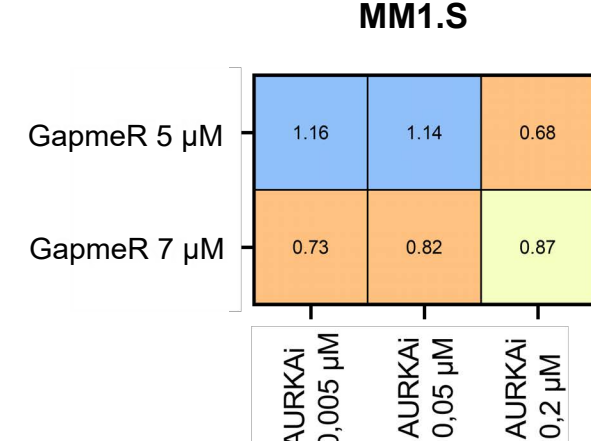
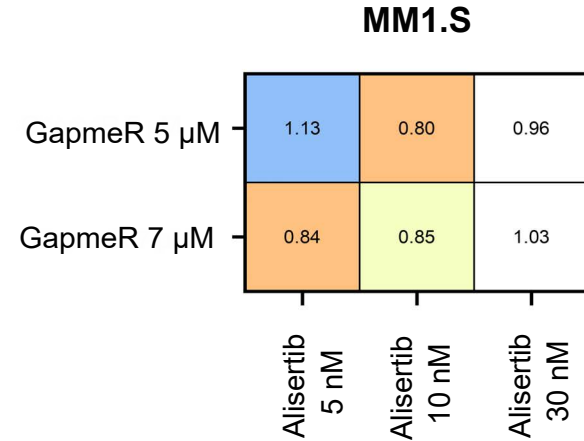
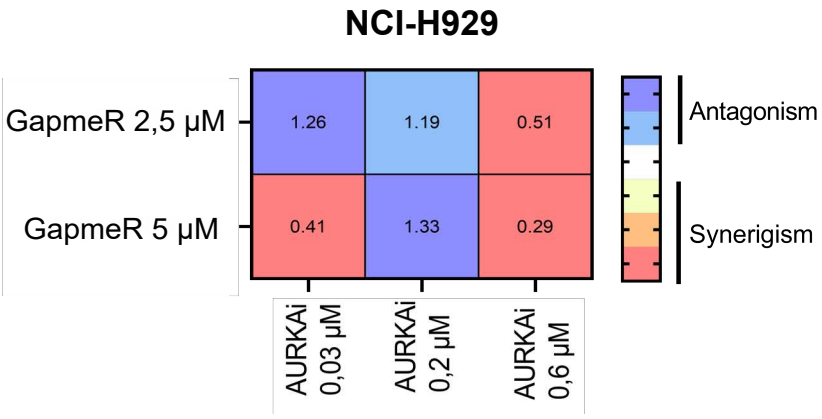
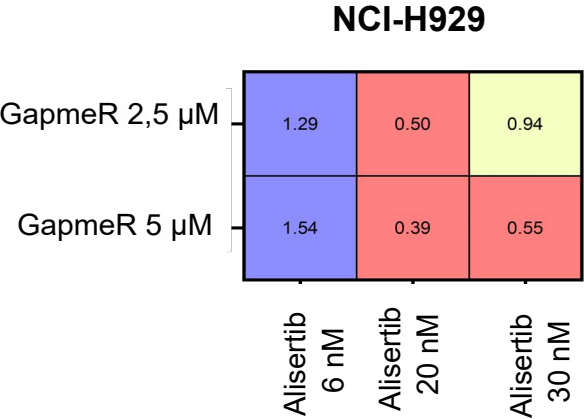
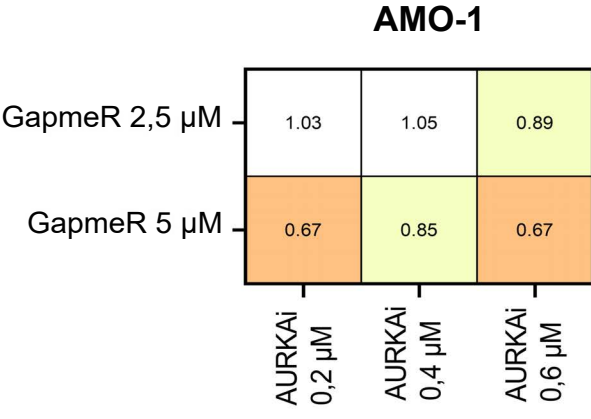


**Supplementary figure 2. Effect of AURKA inhibition on cell cycle.** Representative cell cycle profiles obtained through FACS analysis, of AMO-1, NCI-H929, MM1.S cells after 24 hours of Alisertib (S.2A) and AURKAI-I (S.2B) treatments..

**S.3A**

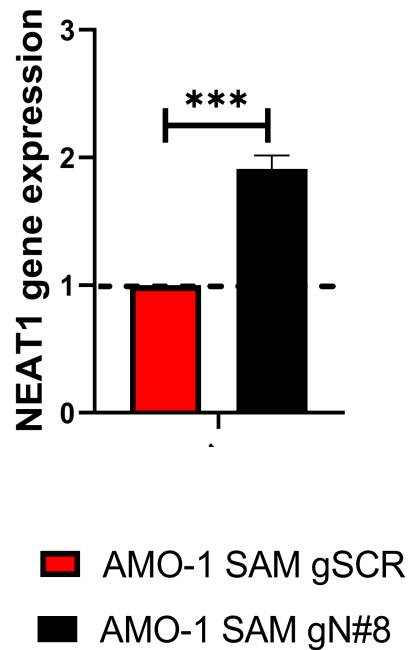


**S.3B**



**Supplementary figure 3. Synergy assessment.** Combination matrix showing combination indexes (CI) resulting from combinatorial treatments of AMO-1, NCI-H929, MM1.S with GapmeR targeting total NEAT1 and Alisertib (S.3A) and AURKAI-I (S.3B) (3-day time point).

## S.4



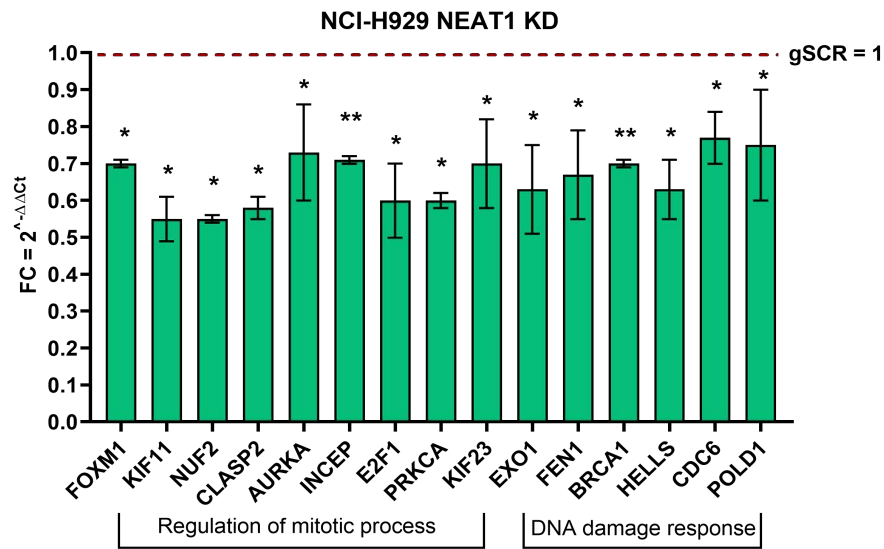
**Supplementary figure 4 (S.4). NEAT1 transactivation in AMO-1 SAM gN#8 cell line.**

Quantitative real time PCR showing NEAT1 expression level in AMO-1 SAM cells.

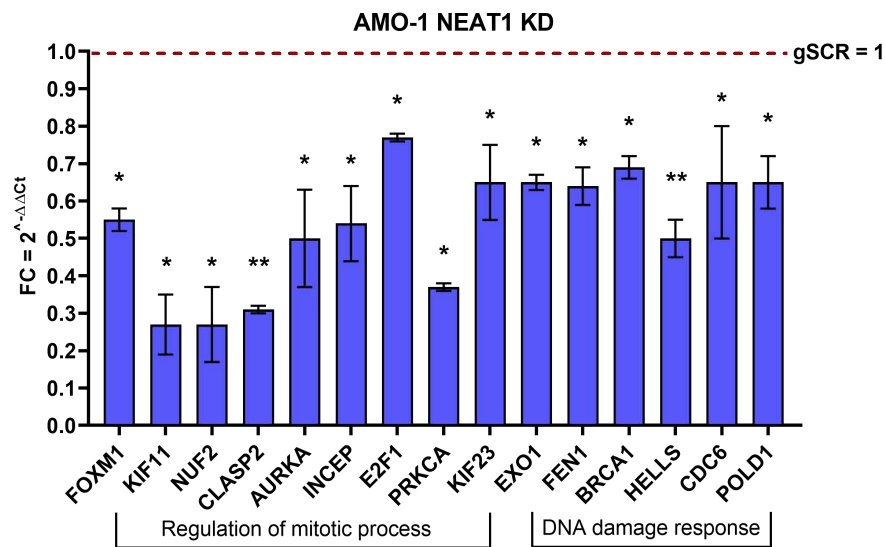
NEAT1 expression was expressed as  $2^{-\Delta\Delta Ct}$ .

Statistical significance was measured with Student's t test.

## S.5A

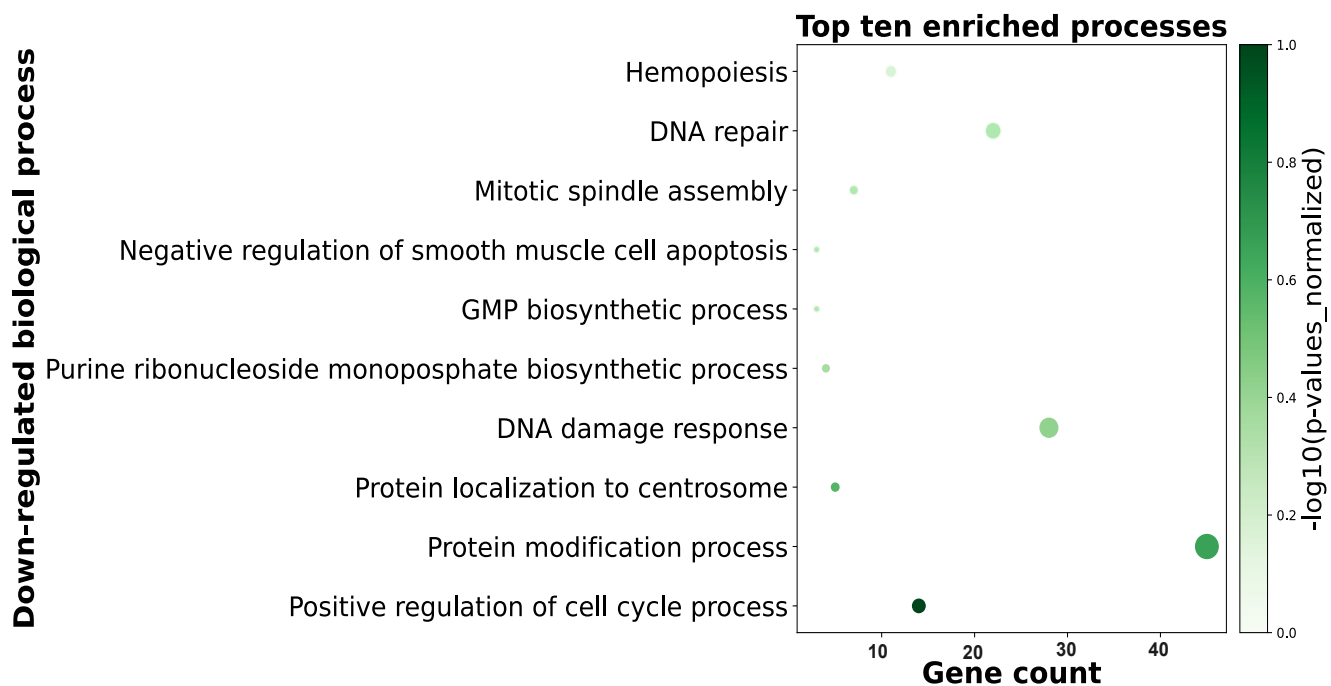


## S.5B



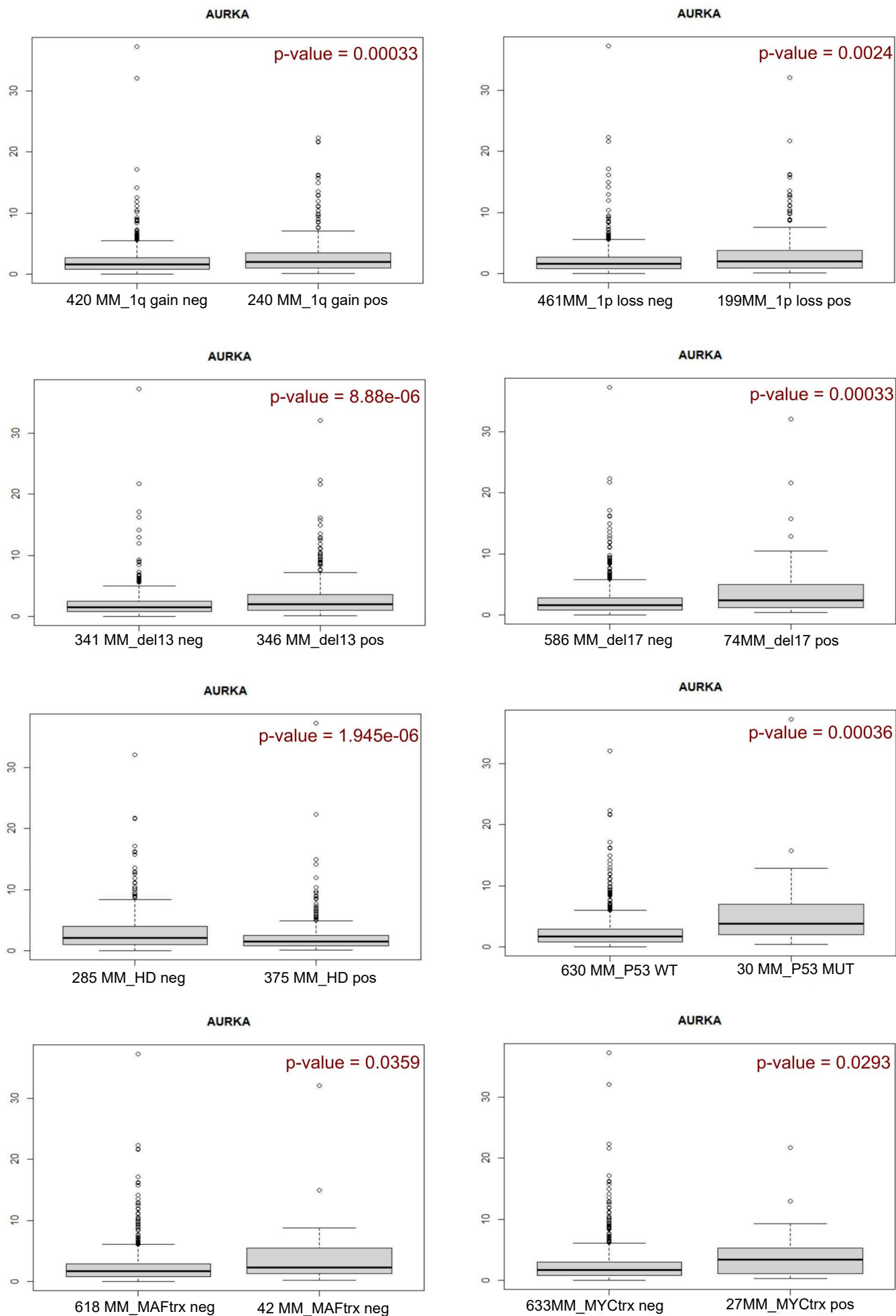
**Supplementary figure 5. Molecular validation of the most significant down-regulated genes in NEAT1 silenced cells.** qRT-PCR validation of differently expressed genes involved in spindle assembly, mitotic regulation and DNA processes in NCI-H929 (S.5A) and AMO-1 silenced for NEAT1 expression (S.5B) following gNEAT1 delivery, compared to scramble condition. (gSCR = 1). Statistical significance was measured with Student's t test.

## S.6



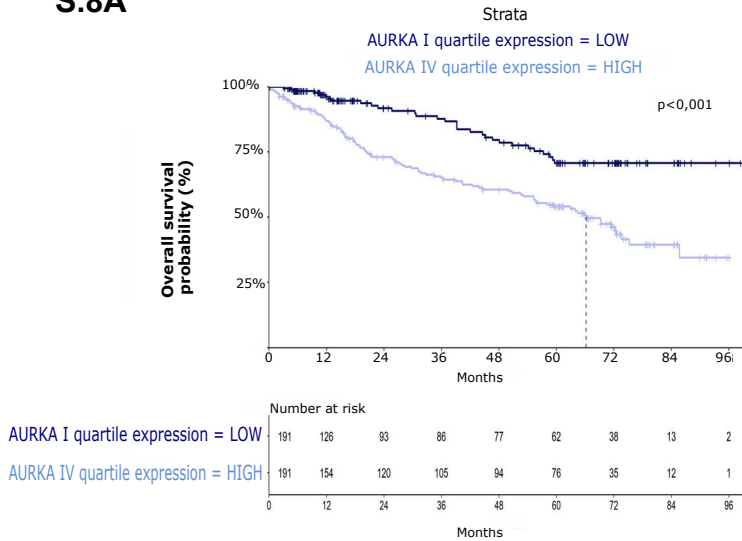
**Supplementary figure 6 (S.6) Gene expression profiling data.** Dot plot of the top ten down-regulated significant biological processes obtained in NCI-H929 NEAT1 KD cells following gNEAT1 delivery.

S.7

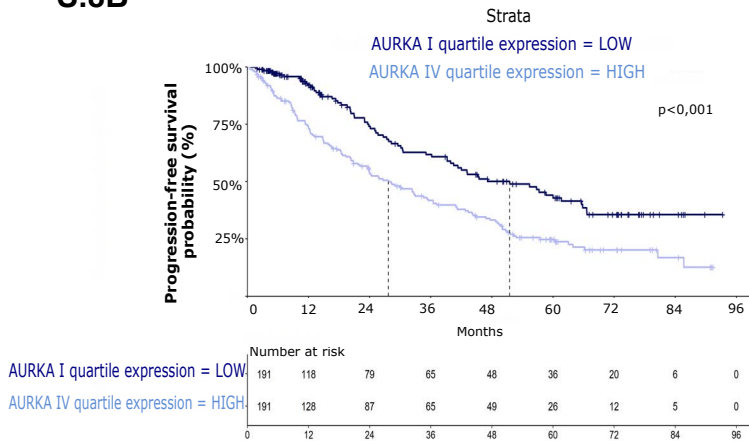


**Supplementary figure 7 (S.7).** Boxplots showing significant differences in AURKA expression in 660MM cases stratified according to the presence of 1q-gain, 1p-loss, del(13q), del(17p), hyperdiploidy (HD), TP53 alterations, MAF and MYC translocation (respectively MAFtrx, MYCtrx). or each plot, differential expression was tested by Wilcoxon rank-sum test with continuity correction. P-values were corrected by BH adjustment.

## S.8A

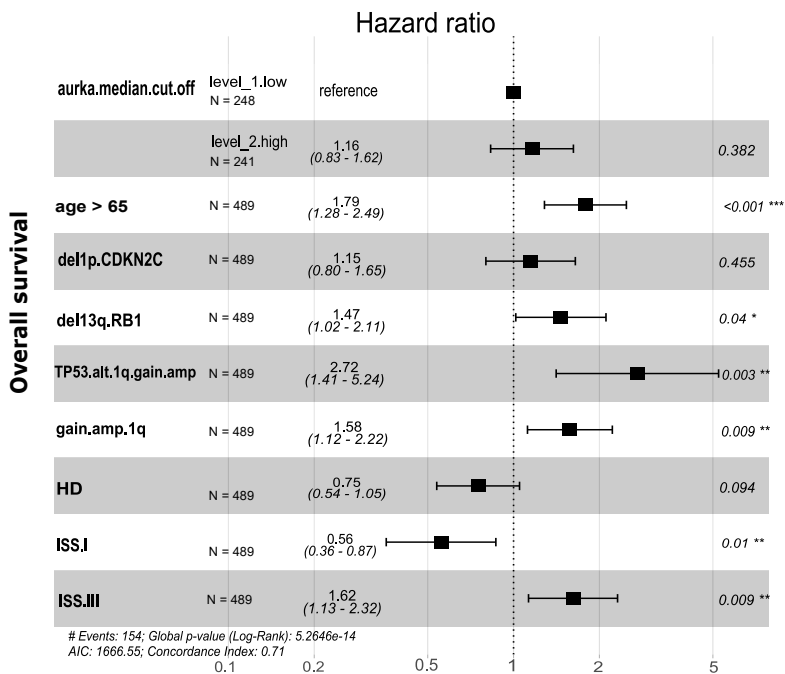


## S.8B

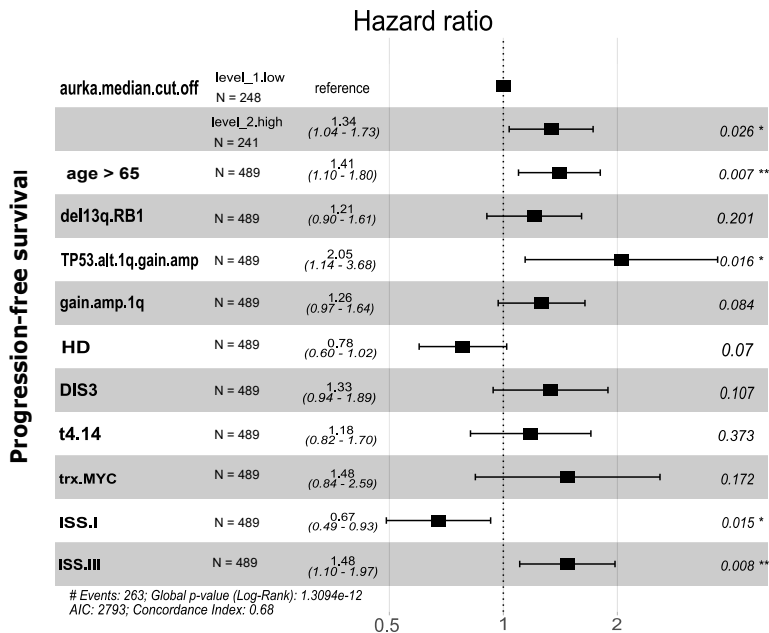


**Supplementary figure 8. Survival analysis.** Overall survival (S.8A) and progression-free survival (S.8B) probability calculated in the CoMMpass dataset which includes 761 patients with MM, stratified in high and low AURKA expression groups, according to quartile, across the dataset. Log-rank test p-value measuring the global difference between survival curves and number of samples at risk in each group across time is reported

**S.9A**

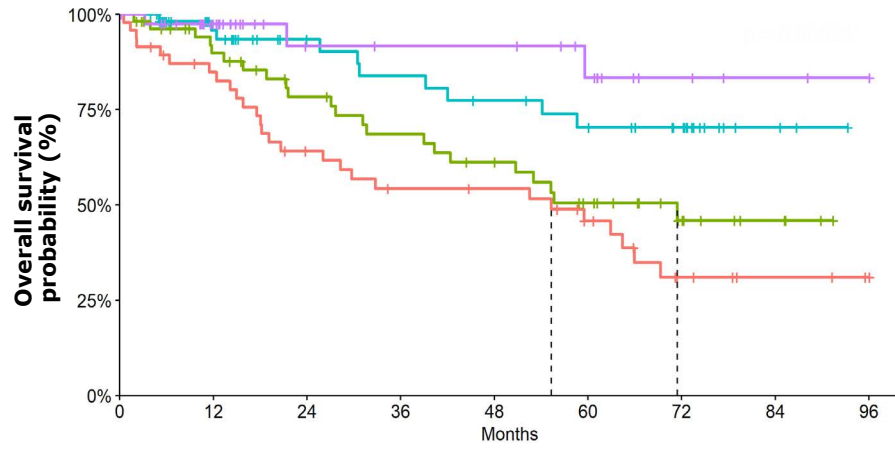


**S.9B**



**Supplementary figure 9. Multivariate analysis.** Forest plots of Cox regression multivariate analyses considering all features with adjusted  $p$ -value  $< 0.05$  in univariate analysis regarding to overall survival (S.9A) and progression-free survival (S.9B), in 489 patients with MM from the CoMMpass cohort. The hazard ratio, 95% confidence interval and P-value are reported for each variable. A global log-rank P-value is reported for each analysis

## S.10



	Number at risk								
	0	12	24	36	48	60	72	84	96
AURKA_High/NEAT1_High	47	37	26	21	20	14	6	3	1
AURKA_High/NEAT1_Low	54	42	33	28	24	17	9	4	0
AURKA_Low/NEAT1_High	56	41	29	26	23	20	14	3	0
AURKA_Low/NEAT1_Low	40	28	15	14	14	10	4	2	1

p value	AURKA_High/NEAT1_High	AURKA_High/NEAT1_Low	AURKA_Low/NEAT1_High
AURKA_High/NEAT1_Low	0,2064	-	-
AURKA_Low/NEAT1_High	0,0028	0,065	-
AURKA_Low/NEAT1_Low	0,0028	0,0226	0,2939

### Supplementary figure 10 (S.10). Effects of AURKA and NEAT1 expression on MM patients survival.

Kaplan-Meier survival curves of 761 patients stratified into four molecular groups based on NEAT1 and AURKA expression, according to quartile, across the CoMMpass dataset. Statistical significance between each curve was reported